

Characterization and use of EBT radiochromic film for IMRT dose verification

Omar A. Zeidan^{a)}

Department of Radiation Physics, M. D. Anderson Cancer Center Orlando, 1400 South Orange Avenue, MP 730, Orlando, Florida 32806

Stacy Ann L. Stephenson

Department of Chemistry and Physics, Wesleyan College, 4760 Forsyth Road, Macon, Georgia 31210

Sanford L. Meeks, Thomas H. Wagner, Twyla R. Willoughby,
Patrick A. Kupelian, and Katja M. Langen

Department of Radiation Physics, M. D. Anderson Cancer Center Orlando, 1400 South Orange Avenue, MP 730, Orlando, Florida 32806

(Received 7 October 2005; revised 8 September 2006; accepted for publication 11 September 2006; published 16 October 2006)

We present an evaluation of a new and improved radiochromic film, type EBT, for its implementation to IMRT dose verification. Using a characterized flat bed color CCD scanner, the film's dose sensitivity, uniformity, and speed of development post exposure were shown to be superior to previous types of radiochromic films. The film's dose response was found to be very similar to ion chamber scans in water through comparisons of depth dose and lateral dose profiles. The effect of EBT film polarization with delivered dose and film scan orientation was shown to have a significant effect on the scanner's OD readout. In addition, the film's large size, flexibility, and the ability to submerge it in water for relatively short periods of time allowed for its use in both water and solid water phantoms to verify TomoTherapy IMRT dose distributions in flat and curved dose planes. Dose verification in 2D was performed on ten IMRT plans (five head and neck and five prostate) by comparing measured EBT dose distributions to TomoTherapy treatment planning system calculated dose. The quality of agreement was quantified by the gamma index for four sets of dose difference and distance to agreement criteria. Based on this study, we show that EBT film has several favorable features that allow for its use in routine IMRT patient-specific QA. © 2006 American Association of Physicists in Medicine. [DOI: 10.1118/1.2360012]

Key words: radiochromic film dosimetry, GAFChromic film, TomoTherapy, diode array, IMRT verification

I. INTRODUCTION

With increasing complexity of intensity-modulated radiation therapy (IMRT) delivery modalities,¹ there is a growing demand for validating delivered dose distributions in multiple dimensions. In this work, we explore the dosimetric properties and implementation of a new radiochromic film (Type EBT, International Specialty Products, Wayne, NJ) for IMRT dose verification. Recent studies on EBT film have focused on studying the film's material characteristics under different exposure conditions and its comparison to other types of radiochromic films (RCFs).^{2,3} However, the implementation of EBT film for dose verification has not been widely addressed in the literature. In addition, little is known about the dosimetric properties of EBT film beyond the manufacturer's product specifications.⁴

In this study, we have examined the most relevant features of this film for its application to IMRT verification in combination with a flat bed document scanner. We have evaluated the quality of the film's measured dose distributions by comparing it to our TomoTherapyTM Hi*Art (TomoTherapy, Inc., Madison, WI) Treatment Planning System (TPS) calculated dose for ten IMRT plans. The gamma index⁵ was used

to quantify the differences between TPS and measured doses for several sets of distance to agreement (DTA) and dose difference (DD) criteria. The film's flexibility combined with the ability to immerse it in water allowed for its use for conventional IMRT QA on curved surfaces.

II. MATERIALS AND METHODS

The new film comes in larger size sheets (20.3 × 25.4 cm²) than any of the previous RCF types (MD-55 and HS, for example), which allows for dose verification over a large area. According to the manufacturer, the film is sensitive in the dose range of 1–800 cGy, making it one of the most sensitive RCF currently available for radiation dosimetry. The manufacturer also specifies that the film reaches OD saturation within 2 h of exposure. The film is flexible enough to allow for shaping into curved surfaces without damage or flaking to the outside protective layer. In addition, the manufacturer's specification⁴ indicates that the film can be submerged in water without permanent damage when immersed for a reasonable amount of time (~1 h), which allows its use in water phantoms without any consequence on its chemical composition.

The EBT film shares some of the characteristics of other types of RCF with respect to sensitivity to environmental factors.^{6–8} Therefore, the film was handled carefully following TG-55 recommendations.⁹ Exposure to fluorescent light was minimized, storing the films in light-tight envelopes. No attempts were made to control temperature and humidity beyond the level of stability provided by the heating and cooling systems of our facility. The films were stored together to avoid differences in thermal histories.

A. Film scanner characterization and image analysis

We have used the Microtek ScanMaker i900 (Microtek International Inc., Hsinchu, Taiwan) 48-bit color charge-coupled-device (CCD) scanner for EBT film digitization. The scanner provides a maximum of 3200×6400 dpi optical resolution with a flat-bed scanning area measuring 20×25 cm². This scanner was characterized for output consistency, sensitivity, linearity, and reproducibility similarly to a previous model.¹⁰ This characterization allowed for the assessment of the utility of this digitizer with or without image processing corrections in combination with EBT model radiochromic film. We preferred to use a flat-bed color CCD transmission scanner in our study over roller-based monochrome CCD scanners such as the widely used Vidar VXR-16 (Vidar Systems Corporation, Herndon, VA) for several reasons: (1) Flat bed scanners generally have better film positional accuracy and reproducibility than roller-based translational scanners.¹⁰ (2) The availability of red channel CCD readout from the Microtek scanner makes it ideal for RCF readout without the need to use red filter coating to optimize readout sensitivity.^{7,11} (3) Small pieces of RCF film can easily be scanned on a flat glass bed scanner without the need to attach them to a larger mask sheet as in the case of the Vidar scanner. (4) In a recent study, Devic *et al.*¹² have shown that color CCD scanners have better readout sensitivity for RCF than monochrome CCD for the same 16 bit signal resolution.

Before any image was acquired, EBT film pieces were firmly placed against the reflective glass to avoid image artifacts from multiple reflections between the film and glass bed. Unless stated otherwise, all images in this study were scanned as raw RGB 48-bit tagged-image-file format (TIFF) in transmission mode at 300 dots per inch (dpi) resolution. Raw images of irradiated films were imported from the scanning system into the Matlab analysis software (Matlab v7.0, Mathworks, Inc.) for further image processing. To reduce inherent image noise, an adaptive 2-D Wiener filter was applied in a 5×5 pixel region to all scanned film images in this study. According to the manufacturer, the absorption spectra of EBT film peaks at 636 nm. Hence, film images were acquired using the scanner's red CCD channel only.

B. Film characterization

The new EBT RCF film was supplied by the manufacturer in a pack of 25 sheets (Lot No. 35076-002AI). We tracked all film pieces in this study by using permanent marker inden-

tations for labeling and to indicate the piece orientation with respect to the initial sheet length/width orientation before it was cut into smaller pieces.

1. Film calibration

Several film pieces from two different sheets were cut to approximately 5×5 cm² and the orientation on each film was marked. The film pieces were then irradiated on a Varian 600C linac (Varian Medical Systems, Palo Alto, CA) to the following doses: 10, 25, 50, 75, 100, 125, 150, 175, 200, 225, 250, 275, 300, 325, 350, 375, and 400 cGy. The films were placed horizontally inside a solid water (Gammex RMI, Middleton, WI) slab phantom of 30×30 cm² size and placed on central axis (CAX) at 10 cm depth. The same calibration measurement was repeated on a different day and the average values of OD from films irradiated to the same dose were recorded. The irradiated film pieces were scanned after 24 h post exposure. The uncertainty in the film measurements was measured as the ratio of standard deviation of the mean OD in a 4×4 cm² region in the middle of the film pieces to the mean OD value in the same region. The net OD was calculated by measuring the OD of the calibration film pieces first and extracting the mean OD value (OD_{base}). OD was measured after exposure ($OD_{measured}$) and net OD for each film was calculated as $netOD (=OD_{measured} - OD_{base})$. A calibrated ion chamber (NEL 2505/3) was inserted in the phantom and below the film plane to check for linac output consistency during film irradiation process and in between the two irradiation measurements.

2. EBT polarization effects

Klassen *et al.*¹³ have shown that measured RCF OD may change substantially due to the polarization of the analyzing light. This effect was attributed to the preferred orientation of the RCF polymer chains, which absorb analyzing light in the microcrystals of the radiosensitive layers. To estimate the effect of film orientation on scanner output for a given dose, four of the calibration film pieces, which measured approximately 5×5 cm² and irradiated to the following doses, 50, 100, 200, and 300 cGy, were digitized at different orientations on the scanning bed. The film pieces were digitized four times in the same location on the scanning bed with the following orientations: 0°, 90°, 180°, and then the film pieces were flipped at the 180° orientation to examine any effects from film face up versus down scan orientation. The mean optical density (OD) for each orientation was then extracted from a common ROI measuring 4.0×4.0 cm² at the center of each image.

3. EBT OD evolution with time—test case

It is desirable to scan exposed RCFs after they have reached a “plateau” in OD gain from self development. To evaluate the film's OD time evolution, a uniform dose of 100 cGy was delivered to two film pieces cut from the same sheet. The purpose of this measurement was to compare relative OD evolution post exposure to the same dose with the

data reported by the manufacturer⁴ and Lynch *et al.*¹⁴ Rink *et al.*² reported that if time is allowed for the radiation-induced polymerization to complete (>2 h), the EBT film does not exhibit dose rate dependencies. We used a dose rate of 250 cGy/min at d_{\max} from a Varian 600C to irradiate the two film pieces at CAX inside a flat solid water phantom. The film pieces were then scanned several times over a period of 4 h, initially at time intervals of several minutes and then once per hour after the first 2 h. For each film, the mean OD was extracted in a ROI measuring approximately 9×10 cm². The average OD values from both films were then used to construct an OD growth curve as a function of time.

4. EBT film uniformity

The ideal RCF dose response when exposed to a uniform irradiation field should be uniform over the exposed area. The uniformity across an entire EBT film sheet was tested indirectly by cutting the film piece into four equally sized sheets measuring approximately 10×12.5 cm². The films were placed horizontally on solid water slab using a 30×30 cm² field at a 100 SSD and 6.0 cm depth with 8 cm back scatter. The film pieces were then irradiated on a 2100C Varian linac using 6 MV nominal energy to the following doses: 50, 100, 150, and 200 cGy. The beam flatness at that depth based on the clinical data for this linac was 1.5%. We used this dose range since it is most relevant to our intended application for verifying single IMRT fraction doses. Dose response uniformity was evaluated by generating 1 mm wide averaged profiles (corresponding to an average of 12 pixel line readings) across the uniformly exposed film image in the horizontal and vertical directions.

5. Comparison of EBT and water PDDs

We compared our TomoTherapy water scan percent-depth-dose (PDD) profile data with CAX profiles from EBT film. Water tank scans were obtained using an A1SL Exradin ion chamber (Standard Imaging, Middleton, WI) with an active volume of 0.056 cm³ and an outside diameter of 6.25 mm. The water surface was set at 85 cm source-surface distance (SSD) and irradiated by a 5×40 cm² field using a 6 MV nominal energy beam. In comparison, a whole EBT film sheet was placed vertically along a cylindrical solid water “cheese” phantom¹ and tightly squeezed between the two halves of the cylindrical phantom pieces using strong Velcro straps. The phantom measured 30 cm in diameter and 18 cm in length. The film surface was set to 85 cm SSD and irradiated with a 40×5 cm² field size. Due to the physical limitations of the cheese phantom, we could only use 18 cm of the length of the film along the beam direction. A 1 mm wide averaged profile from the exposed film was generated at CAX and compared to water scan data.

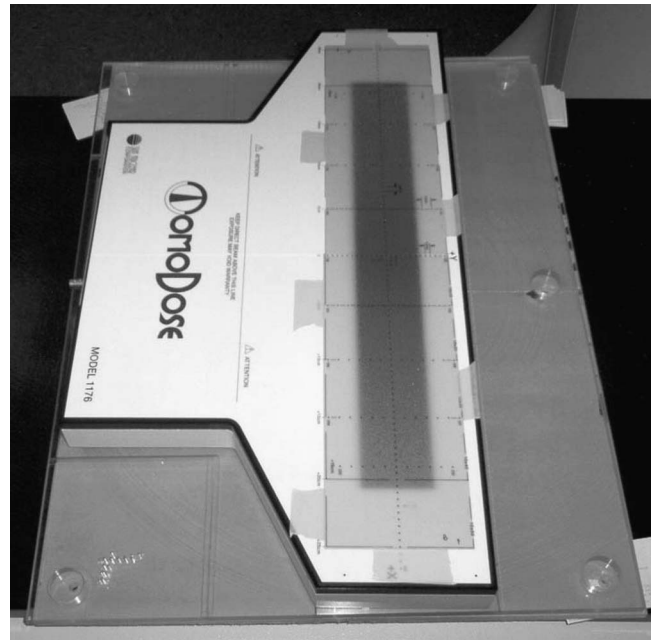


Fig. 1. A picture of the TomoDOSE™ diode array showing EBT film pieces post irradiation on top of the array.

6. Comparison of EBT dose profiles to diode array profiles

We tested the accuracy of the film lateral dose profiles using the TomoDOSE™ diode array detector (Sun Nuclear, Melbourne, FL). The array consists of 107 diodes arranged in a row along the lateral axis located with 5 mm diode to diode spacing. The diode array was shown to reproduce lateral dose profiles from ion chamber water tank scans based on recent work from our group.¹⁵ Diode array measurements were performed for a 5×40 cm² field at several depths. To cover this large field size with EBT film, two identical pieces of the film were cut from the same sheet and abutted directly on top of the diode array as shown in Fig. 1. Each film piece measured approximately 10 cm in width and 25 cm in length. A sheet of solid water with a thickness of 1.5 cm and 15×55 cm² in width and length was used as build up. The film pieces were then irradiated with a field size of 5×40 cm² to 267 cGy.

C. Phantom IMRT measurements and dose verification analysis

1. Solid water phantom plan deliveries and verification analysis

Sheets of EBT film were placed inside the cylindrical solid water phantom in a plane perpendicular to the gantry rotation plane. We delivered a total of ten IMRT hybrid plans (five head and neck (H & N) and five prostate) and compared measured with calculated dose distributions from TomoTherapy TPS (version 2.1.1a). The dose was calculated in the phantom using a 1.9 mm pixel dose resolution. Each film was marked with four points corresponding to the green lasers (virtual isocenter) in the coronal plane for image regis-

tration. The irradiated film pieces were digitized at a resolution of 72 ppi ($0.35 \times 0.35 \text{ mm}^2$). The calculated dose distributions were exported from the TPS and then up-sampled in Matlab using nearest neighbor interpolation to match the film's measured dose grid resolution. A mean dose value was calculated inside a region of low-gradient, high dose distribution and measuring approximately $10 \times 10 \text{ mm}^2$ to which both dose distributions were normalized. The two dose distributions were then registered based on the position of the virtual isocenter of each plan (corresponding to the positions of the green lasers). Each dose distribution was normalized to the same dose point pixel in a region with maximum dose. The gamma index⁵ was used as an indicator of the agreement quality between measured and calculated dose distributions. Gamma values in 2D were calculated in a common ROI for the coregistered and normalized dose distributions for different DD and DTA criteria. The following sets of criteria 2 mm and 2%, 4 mm and 3%, and 3 mm and 5%, were used for gamma index evaluation based on various recommendations in the literature.^{16–18} In addition, we added our own criteria of 3 mm and 3%. The gamma calculation search radius was set to 1.0 cm with no calculations performed within 1.0 cm from the edge of the ROI. The ROI for each plan was chosen such that it extends to include regions with 30% isodose line and higher. These rectangular ROIs measured on average nearly $206 \times 114 \text{ mm}^2$ and $218 \times 157 \text{ mm}^2$ for prostate and H&N plans, respectively.

2. Water phantom plan deliveries and verification analysis

The flexibility of EBT film combined with its design to be handled in room light gives freedom to the user to manipulate and position the film precisely in nonplanar surfaces and in both solid or real water phantoms. Previous attempts to acquire 3D subspace dose information film dosimetry^{19,20} involved the use of EDR2 silver-halide film in a spiral phantom. That process required precise placement of the film tightly inside the phantom and working in a dark room before and after phantom irradiation. In this measurement, we demonstrated that these favorable features of EBT film have enabled us to use it nonconventionally to verify dose in a cylindrical plane and in real water phantoms. To demonstrate that the film's OD is relatively insensitive to reasonable submersion times in water, we used one of the uniformity films that was previously irradiated to 100 cGy. The dimensions were $10 \times 12.5 \text{ cm}^2$ and OD was measured at the center of the film before and after submersion in water for half an hour. The amount of time it took us to perform the film IMRT measurement in a real water phantom was slightly less than 30 min. We used a cylindrical phantom geometry since it is most natural for dose verification on a TomoTherapy unit. The cylindrical phantom was constructed in house from a thin plastic sheet wrapped in the shape of a cylinder and placed in a reproducible position at the center of a rectangular transparent plastic container using fixation plates at the two ends of the cylinder. The sides of the container and the front and back were marked with fiducial cross wires for

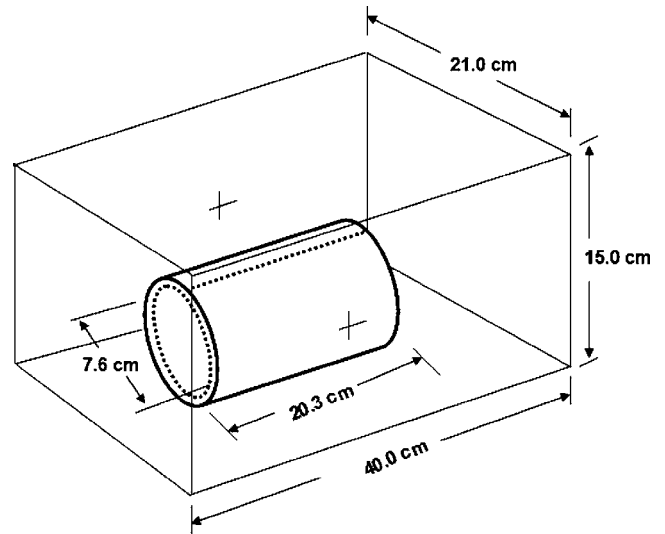


FIG. 2. A schematic of the cylindrical phantom setup. The dotted line represents the location of the EBT film sheet.

laser alignment. The film was cut to fit tightly on the inside surface of the cylinder as shown in Fig. 2. The film was first wrapped in a thin Mylar sheet to prevent scratching the film against the inside of the cylinder surface when inserting and extracting the film from the cylinder. Point marks were placed at the edges and corners of the film to indicate the orientation and position with respect to the outside surface markers. Water was added to fill the entire container and inside of the cylinder up to 2 cm above the cylindrical surface. The whole phantom was then scanned on our CT scanner without the EBT film and the data were exported to TomoTherapy TPS for dose calculation. One H&N plan from the flat 2D IMRT verification measurement was recalculated with the finest available dose grid ($1.9 \times 3.0 \text{ mm}^2$) onto the new phantom geometry. The 3D dose information was then exported from the TPS in binary format for analysis. Although other types of RCF were used previously in water phantoms,²¹ this is the first time to our knowledge that this new type of RCF has been used in water for nonplanar IMRT dose verifications.

III. RESULTS

A. Scanner characterization

The linearity of the scanner against OD was checked using a standard Kodak step tablet (SN 607ST153). The tablet had 20 steps with OD values ranging from 0.04 to 2.86. We found that the measured $\text{OD} = -\log_{10}(S/2^{16})$, where S is the scanner's pixel raw transmission reading through the EBT film on the glass bed, exhibits a strong linear relation with the standard Kodak OD values up to OD of 1.2. Measured EBT OD values from all film exposures in this study were well within this linear range. It is worth mentioning that the transmission value S from our scanner for any EBT film piece preexposure was constant at 6154 (which translates to an OD value of 0.027). The measured dose uncertainty ($=$ standard deviation/mean) for this OD was 3%. This OD

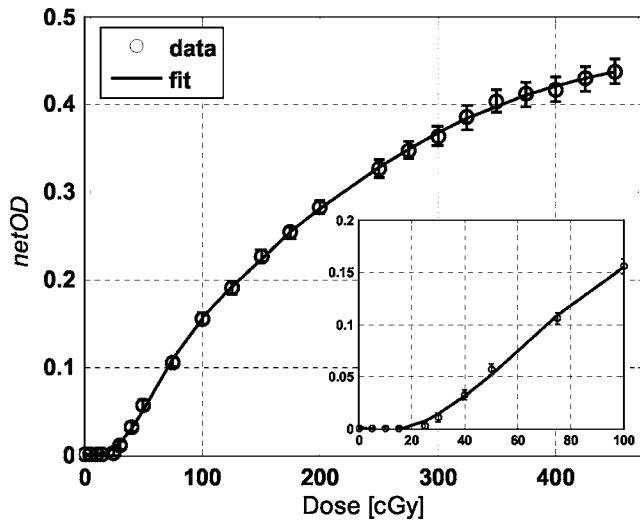


FIG. 3. EBT film calibration curve. The zoom-in insert shows low-dose data points. Error bars represent uncertainties in measured OD.

value represents the ratio of the scanner transmission value when the unexposed film is placed on the flat bed scanner over the transmission value of the glass bed only ($S=2^{16}$). Since this background signal was consistent throughout the study, we decided not to correct for it in the acquired scanner images. The scanner output was also checked for output consistency with time and OD using a standard Kodak step tablet (Q-60E1). For each scan, the tablet was placed on the same position on the flat bed scanner and digitized over a period of 10 consecutive days. The scan from each day was analyzed and the mean value of each step was extracted. The scanner-measured OD had reproducibility errors within 3% for OD values as low as 0.05 and within 0.5% for OD of 0.950 and higher.

B. Film characterization

1. Film calibration

A plot of the EBT calibration curve of averaged *netOD* from both calibration measurements with respect to delivered dose is displayed in Fig. 3. OD values from both measurements were very reproducible and well within 2% from each other for any dose value over the entire delivered dose range shown in Fig. 3. No detected change was observed in the linac output during or in between the calibration measurements. The fitted curve, represented by the solid line, is composed of two separate third-order polynomial fits, one for the low-dose region and another one for the rest of the data points. The two curves were met at the 100 cGy dose point. A dose uncertainty of 3% was measured for the lowest film doses between 5 and 25 cGy. The low dose data from Fig. 3 show that our scanner could not distinguish OD below 25 cGy (i.e., for all doses below that value an OD of 0.027 was measured). For the sake of comparison, one can use this calibration curve to compare the net OD of EBT with other types of RCF.²² For example, to obtain a net OD of 0.3 requires a dose value of 321 cGy for RCF type HS and 890 cGy for MD55-2, respectively. In comparison it takes

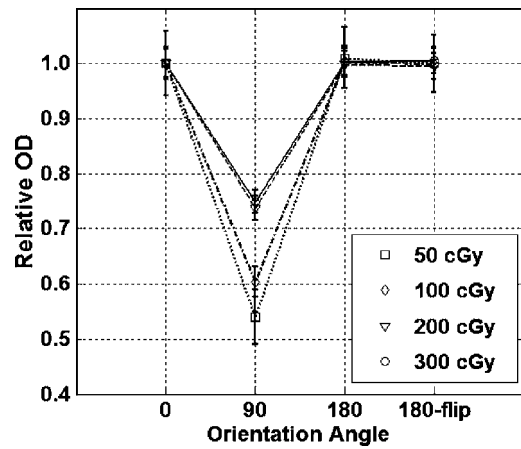


FIG. 4. The effect of EBT film polarization with delivered dose on OD readout and film scan orientation. Relative OD values are normalized to the zero orientation OD. Error bars represent measured OD uncertainties.

only 220 cGy for EBT to reach a net OD of 0.3 based on the calibration curve in Fig. 3.

2. Polarization effects

Figure 4 displays relative measured OD against film orientation on the scanning bed for four delivered dose values. OD values per orientation were normalized to the initial OD value at the initial 0° orientation. The 0°, 180°, and 180° flip orientations are nearly equivalent for most of the doses shown in Fig. 4. There is a dose-dependent effect at the 90° orientation where the measured OD drops from the 0° orientation by nearly 50% for 50 cGy dose to 25% for 200 cGy or higher doses. This orientation effect is nearly four times larger than what was previously reported for other types of RCF.¹³ Due to this large fluctuation in scanner output response with film orientation, we have maintained either the 0° or 180° orientation scans for all films in this study. The pronounced light polarization effect of EBT film could be attributed to the structure of the active layer of this new radiochromic film. Rink *et al.*² have shown that the monomer layers in EBT are elongated, sticklike structures compared to MD-55 sandlike monomer crystals.

3. EBT OD evolution

The EBT film post-exposure OD growth with time is demonstrated in Fig. 5. The OD growth seems to stabilize after nearly 100 min, which is in good agreement with a recent work.¹⁴ This measurement was essential to give us an indication of how fast the film reaches its OD growth plateau post exposure to a uniform dose. Although film development rate is dependent on delivered dose and dose rate,^{2,14} we have decided to wait nearly 24 h post exposure before reading all our films to guarantee full development and exclude any potential OD growth-dependent factors from delivered dose and dose rate.

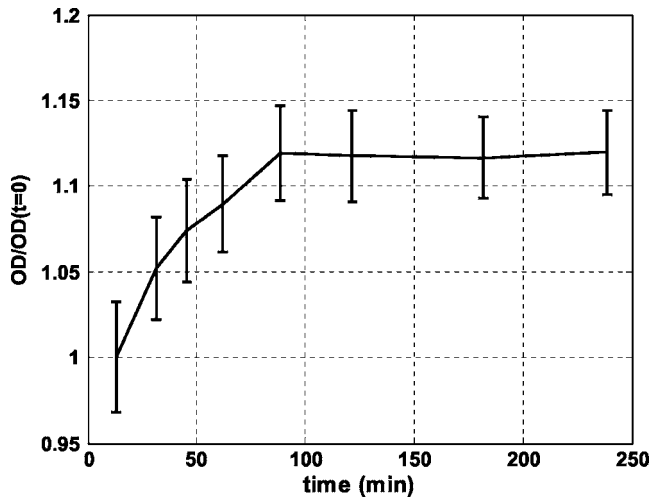


FIG. 5. EBT film OD with time post uniform irradiation to 100 cGy dose. Error bars represent the measured OD uncertainties.

4. EBT dose uniformity

Figure 6 displays four plots of averaged horizontal and vertical 1 mm thick profiles across the film. The OD profiles were taken at the center of each film and then normalized by the average pixel values over a central 1 cm long strip of the profile. It is clear from Fig. 6 that the relative uniformity of the film improves with dose, for example $\pm 4\%$ for 50 cGy to

$\pm 1.5\%$ for 200 cGy. The uniformity of this film based on a single exposure is much better than previous types of RCF, where nonuniformities larger than 10% were measured even after uniform dose exposures on the order of 1000 Gy or higher.^{13,23–25} Hence, to suppress the large effects of nonuniform RCF response, a double exposure technique was developed.²³ The new EBT film shows superior dose response uniformity compared to other types of RCF film. Therefore, we decided that it is not necessary to implement the double exposure technique with this film.

5. Comparison of EBT and water PDDs

A profile overlay of measured PDDs from water scan data and EBT film is shown in Fig. 7. Both profiles were normalized to the d_{\max} profile value. The ratio of the two profiles as shown in the insert of Fig. 7 indicates that the film profile reproduces the water scan profile to within $\pm 4\%$ for most of the measured depth. This agreement between the two profiles indicates that EBT film relative dose response is similar to water and shows no apparent sensitivity to beam hardening with depth.

6. Comparison of EBT dose profiles to diode array profiles

Figure 8 displays an overlay plot of profiles from EBT film and the diode array profiler. The 1 mm thick film aver-

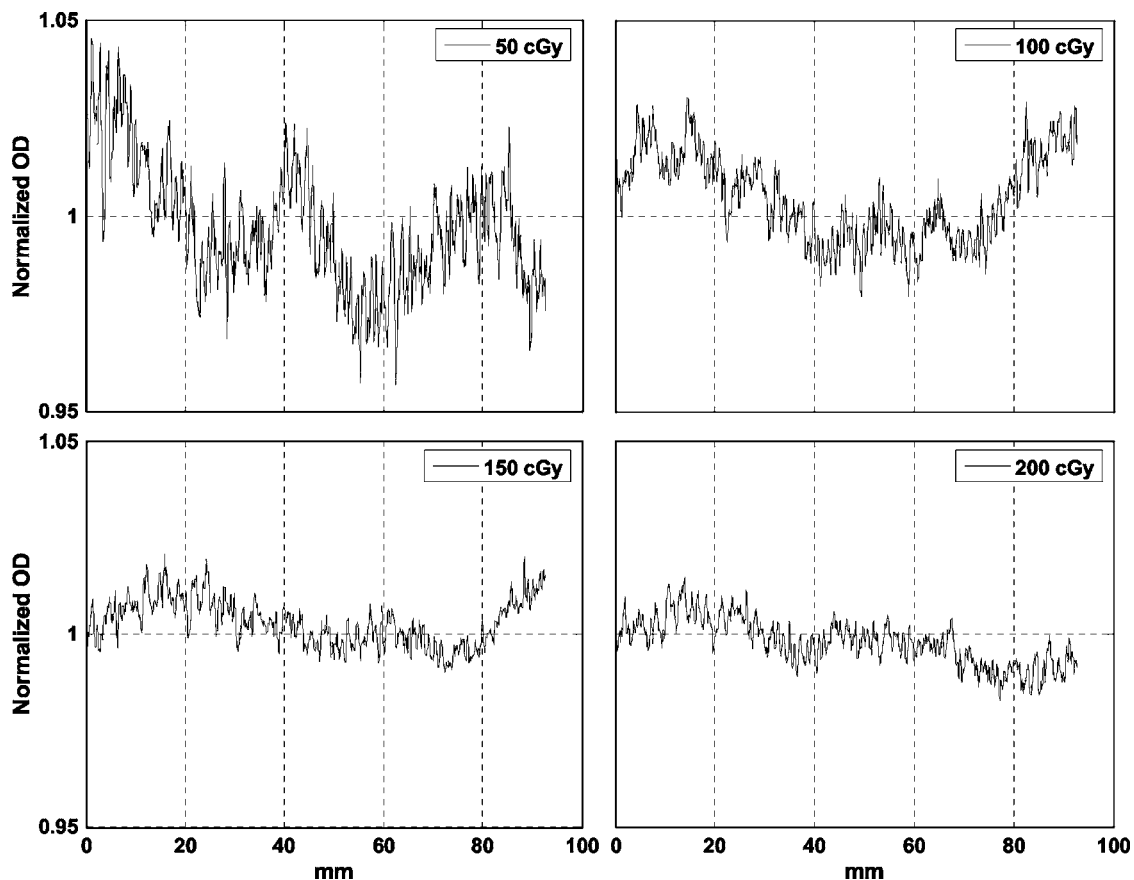


FIG. 6. Averaged horizontal and vertical normalized dose profiles across EBT film post exposure to uniform dose in the range 50–200 cGy.

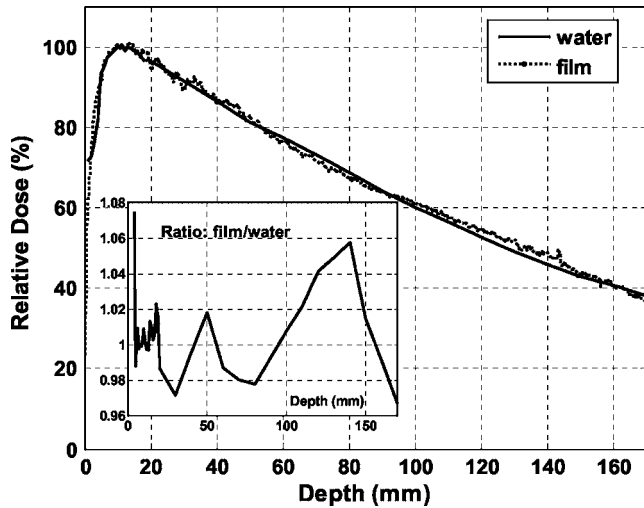


Fig. 7. An overlay of water and EBT film PDDs for a 5×40 cm² TomoTherapy radiation field. The insert displays the ratio of both PDDs.

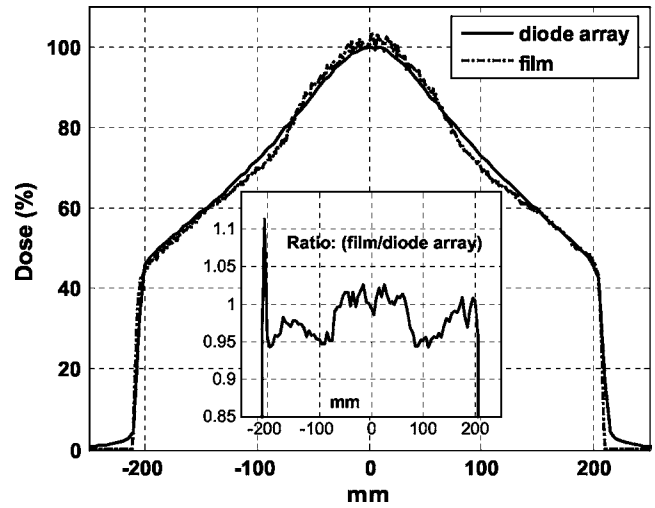


Fig. 8. An overlay of TomoDOSE™ diode array and EBT film lateral dose profiles. The film was placed at a depth of 1.5 cm in a solid water phantom and at 85 cm SSD. The insert displays the ratio of both profiles.

aged profile was taken at the center of the film and at the location of the position of the profiler detectors. The profile overlay clearly shows that EBT film can accurately describe the lateral dose fall-off for the beams produced from our largest field opening on our TomoTherapy unit. The insert in Fig. 8 shows that the relative film profile falls within ±5% from the diode array profile for most of the profile spatial range. Due to OD threshold sensitivity of our scanner, the film response to low doses in the penumbra is reflected as a flat response and does not reproduce the diode data below the 5% (13 cGy) of penumbra dose (267 cGy).

C. IMRT measurements and analysis

1. Dose verifications on a flat plane

The first four rows of Table I show the percentage of pixels passing four gamma criteria (gamma value ≤1.0) for all ten IMRT plans. The first five plans are prostate and the last five are H&N plans. The higher the passing percentage the better the agreement between calculated and measured dose distributions. The overall agreement was better as the criteria tolerance increased. The percentage of dose pixels passing all ten IMRT cases per criteria was 67±9% for the 2 mm and 2% criteria, 87±8% for the 3 mm and 3% criteria, 90±7% for the 4 mm and 3% criteria, and 96±4% for the 3 mm and 5% criteria. These percentages are comparable to

a recent study using the same modality and measurement technique but using EDR2 film for dose verification.²⁶ This similarity between EBT and EDR2 based on gamma index analysis indicates that EBT film is a suitable alternative for routine IMRT QA to the well established EDR2 film. The bottom row of Table I list absolute percent differences between measured and calculated doses for each IMRT plan inside a ROI of maximum uniform dose. The mean and standard deviation of these differences were found to be 3±1%.

An example of isodose contours and a dose profile overlay from EBT and TPS as a result of the irradiation of a hybrid H&N plan is shown in Fig. 9. The two dose distributions were normalized to the same ROI of 1.0×1.0 cm² inside of a maximum uniform dose region. The length and direction of the dose profile from both TPS and EBT image in Fig. 9(b) correspond to the length and direction of the arrow in Fig. 9(a). The point dose value from the TPS to the point of ion chamber measurement for a single fraction was 1.331 Gy and from measurement was 1.369 Gy, which yields an acceptable dose difference of less than 3%.

2. Dose verification on a cylindrical plane

We found an insignificant difference (~0.5%) between the OD of the EBT film piece before and after water submersion. In addition, we observed a separation or “flaking” in

TABLE I. Percentage of pixels passing four different gamma index criteria for ten IMRT treatments plans. The absolute percentage difference between measured and calculated doses inside a ROI of maximum uniform dose is listed in the bottom row.

Plan	1	2	3	4	5	6	7	8	9	10
2 mm and 2%	69.8	83.6	60.5	58.7	71.4	69.5	73.3	69.1	46.3	64.1
3 mm and 3%	90.3	98.1	81.2	80.9	89.2	91.8	94.6	88.6	69.1	84.2
4 mm and 3%	93.1	98.7	86.4	84.4	91.3	94.0	97.9	90.8	73.7	89.0
3 mm and 5%	99.3	100.0	94.4	92.6	97.6	99.6	99.2	96.1	86.9	95.4
Difference (%)	4.7	3.1	2.3	4.5	4.7	2.1	1.3	1.4	4.8	3.2

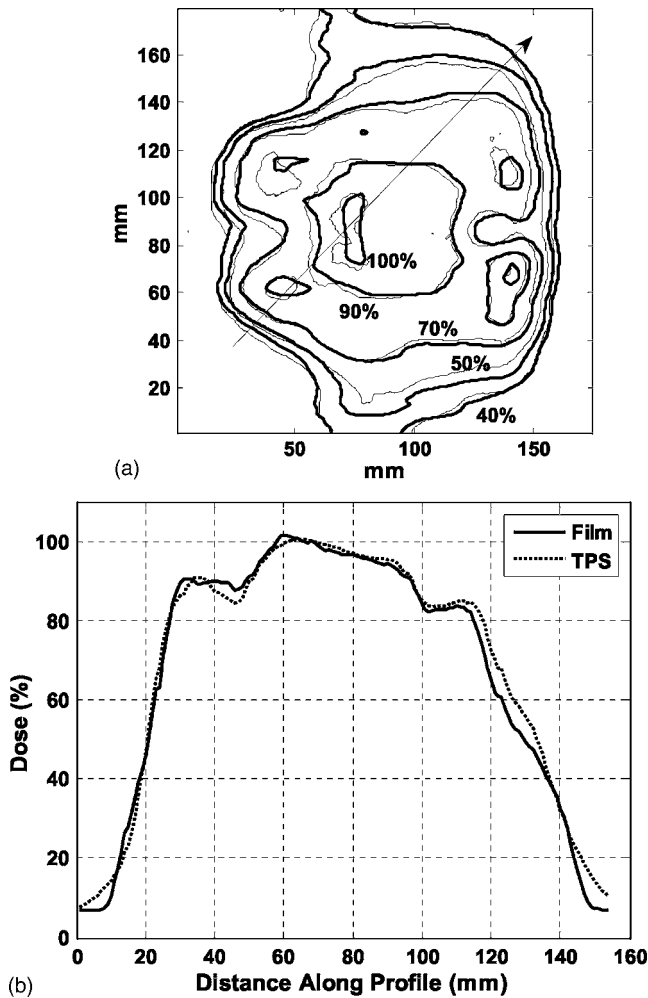


FIG. 9. (a) An overlay of normalized isodose contours from calculated TomoTherapy and EBT film dose distributions of a H&N hybrid IMRT plan delivery on a flat slab solid water phantom. The thin contours represent the film isodose distribution and the thick contours represent the TPS isodose distributions. (b) Normalized profiles of TomoTherapy TPS and EBT film taken across the isodose distribution as shown by the arrow in (a).

the film edges in the order of 2–3 mm after the submersion, which was due to water diffusion in between the protective polyester layers. Calculated and EBT isodose contours and a dose profile overlay from irradiation of the same hybrid H&N plan above in the cylindrical water phantom are displayed in Fig. 10. The two dose distributions were normalized to the same ROI of $1.0 \times 1.0 \text{ cm}^2$ inside of a maximum uniform dose region. The dose profile from TPS and EBT in Fig. 10(b) are generated similarly to Fig. 9(b). A maximum relative difference of 5% was measured between the two profiles. The overall dose agreement between film and TPS dose distributions is acceptable. There is a slight discrepancy between the contours for the 50% isodose line at the far right end of the dose distributions in Fig. 10(a). This discrepancy is located at the junction where both ends of the film abut to close the cylindrical loop. Due to the film's elastic force, the film ends at the junction slightly bulge outwards and away from the inside surface of the cylindrical phantom, hence causing this apparent discrepancy with the TPS.

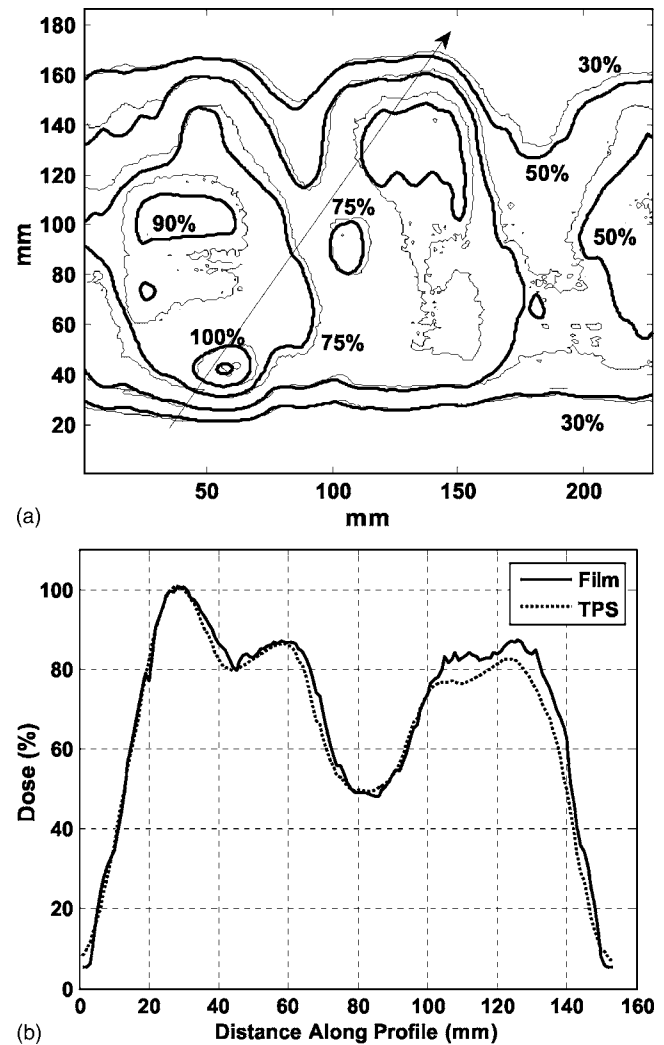


FIG. 10. (a) An overlay of normalized isodose contours from TomoTherapy TPS and EBT film dose distributions of a H&N hybrid plan delivery on the cylindrical phantom. The thick contour represents the TPS isodose distribution and the thin contour represents the film isodose distribution. (b) Normalized profiles from TomoTherapy TPS and EBT film taken across the isodose distribution as shown by the arrow in (a).

IV. DISCUSSION AND CONCLUSIONS

This study addresses the dosimetric features of a new and improved radiochromic film and demonstrates its use in conjunction with a flat-bed scanner for IMRT single fraction verifications. The scanner was first characterized to insure its ability to generate high-quality, high-resolution images with minimal or no image artifacts. The film's intrinsic polarization was shown to be a function of delivered dose and could affect digitized image output by as much as 50%. Therefore, it is important to use a consistent film orientation on the scanning bed to insure image readout consistency. The study of EBT OD time evolution indicates that the film fully develops nearly 2 h post exposure, making it one of the fastest developing GAFChromic films. Dose uniformity of the film was shown to improve with higher dose exposures and can attain an overall uniformity level of $\pm 1.5\%$ when exposed to a uniform dose of 200 cGy. The new film showed a detect-

able OD response for doses as low as 25 cGy as resolved by the scanner used in this study. EBT film dose response with depth was shown to reproduce water scan relative depth doses to within $\pm 4\%$ and lateral relative dose profiles to within $\pm 5\%$. The EBT film was shown to produce acceptable agreements between calculated and measured dose distributions by analyzing ten IMRT plans for four different sets of acceptance criteria of the gamma index. The percentages of pixels passing these criteria were comparable to EDR2 film based on a recent work²⁵ using the same modality and measurement technique. The percent differences between measured and calculated doses for each IMRT plan inside a ROI of maximum uniform dose was within $\pm 5\%$.

Finally, we have exploited some of the attractive features of this film such as its large size, flexibility, and relative insensitivity to water to use it in a real water phantom for IMRT verification. We have shown that there is an insignificant effect on the film's OD readout if the film is submerged in water for up to 30 min. By shaping the film in a cylindrical column inside a water phantom, we have demonstrated that single IMRT dose fractions can be verified on a curved plane. We are currently in the process of establishing a routine use of this film for IMRT verification as part of our patient-specific QA.

ACKNOWLEDGMENTS

Special thanks to Todd Gilbert for his help in constructing the cylindrical phantom, to the American Association of Physicists in Medicine for their support of Stacy Ann Stephenson through the Summer Undergraduate Fellowship Program, and to Women Playing for T.I.M.E for their support of our research program.

^{a)}Electronic mail: Omar.zeidan@orhs.org

¹T. R. Mackie *et al.*, "Helical Tomotherapy," in *Intensity Modulated Radiation Therapy: The State of the Art*, AAPM Summer School Proceedings (2003) pp. 264–284.

²A. Rink, I. A. Vitkin, and D. Jaffray, "Characterization and real-time optical measurements of the ionizing radiation dose response for a new radiochromic medium," *Med. Phys.* **32**(8), 2510–2516 (2005).

³S. Devic, J. Seuntjens, E. Sham, and E. B. Podgorsak, "Precise radiochromic film dosimetry using a flat-bed document scanner," *Med. Phys.* **32**, 2245–2253 (2005).

⁴"GAFCHROMIC EBT white paper," International Specialty Products (ISP), <https://www.ispcorp.com/products/dosimetry/index.html>

⁵D. Low, W. Harms, S. Mutic, and J. Purdy, "A technique for the quantitative evaluation of dose distributions," *Med. Phys.* **20**, 1709–1719 (1993).

⁶L. E. Reinstein and G. R. Gluckman, "Predicting optical densitometer response as a function of light source characteristics for radiochromic film dosimetry," *Med. Phys.* **24**, 1935–1942 (1997).

⁷A. Rink, I. A. Vitkin, and D. Jaffray, "Suitability of radiochromic medium for real-time measurements of ionizing radiation dose," *Med. Phys.* **32**, 1140–1155 (2005).

⁸M. L. Butson, T. Chueng, P. K. N. Yu, and P. E. Metcalfe, "Effects of read-out light sources and ambient light on radiochromic film," *Phys. Med. Biol.* **43**, 2407–2412 (1998).

⁹A. Niroomand-Rad *et al.*, "Radiochromic film dosimetry: Recommendations of AAPM Radiation Therapy Committee Task Group 55," *Med. Phys.* **25**, 2093–2115 (1998).

¹⁰O. A. Zeidan and J. F. Dempsey, "Characterization of an inexpensive transmission color linear-CCD array film digitizer for IMRT dosimetry," *Med. Phys.* **29**, 1265 (2002).

¹¹D. O. Odero, G. R. Gluckman, K. Welsh, R. A. Wlodarczyk, and L. E. Reinstein, "The use of an inexpensive red acetate filter to improve the sensitivity of GAFChromic dosimetry," *Med. Phys.* **28**, 1446–1448 (2001).

¹²S. Devic, J. Seuntjens, G. Hegyi, E. B. Podgorsak, C. G. Soares, A. S. Kirov, I. Ali, J. F. Williamson, and A. Elizondo, "Dosimetric properties of improved GafChromic films for seven different digitizers," *Med. Phys.* **31**, 2392–2401 (2004).

¹³N. V. Klassen and L. van der Zwan, "GafChromic MD-55: Investigated as a precision dosimeter," *Med. Phys.* **24**, 1924–1934 (1997).

¹⁴B. Lynch, M. Ranade, J. Li, and J. Dempsey, "Characteristics of a new very high sensitivity radiochromic film," *Med. Phys.* **31**, 1837 (2004).

¹⁵K. M. Langen, S. L. Meeks, D. O. Poole, T. H. Wagner, T. R. Willoughby, O. A. Zeidan, P. A. Kupelian, K. J. Ruchala, and G. H. Olivera, "Evaluation of a diode array for QA measurements on a helical tomotherapy unit," *Med. Phys.* **32**, 3424–3430 (2005).

¹⁶ICRU 42, "Use of computers in external beam radiotherapy procedures with high-energy photons and electrons," 1987.

¹⁷J. Van Dyke *et al.*, "Commissioning and QA of treatment planning computers," *Int. J. Radiat. Oncol., Biol., Phys.* **26**, 261–273 (1993).

¹⁸P. Winkler *et al.*, "Performance analysis of a film dosimetric quality assurance procedure for IMRT with regard to the employment of quantitative evaluation methods," *Phys. Med. Biol.* **50**, 643–654 (2005).

¹⁹S. L. Richardson, W. A. Tomé, N. P. Orton, T. R. McNutt, and B. R. Paliwal, "IMRT delivery verification using a spiral phantom," *Med. Phys.* **30**, 2553–2558 (2003).

²⁰B. Paliwal, W. A. Tomé, S. Richardson, and T. Rockwell Mackie, "A spiral phantom for IMRT and tomotherapy treatment delivery verification," *Med. Phys.* **27**, 2503–2507 (2000).

²¹M. L. Butson, T. Chueng, and P. K. N. Yu, "Radiochromic film dosimetry in water phantoms," *Phys. Med. Biol.* **46**, N27–N31 (2001).

²²O. A. Zeidan, J. G. Li, D. A. Low, and J. F. Dempsey, "Comparison of small photon beams measured using radiochromic and silver-halide films in solid water phantoms," *Med. Phys.* **31**, 2730–2737 (2004).

²³Y. M. Zhu, A. S. Kirov, V. Mishra, A. S. Meigooni, and J. F. Williamson, "Quantitative evaluation of radiochromic film response for two-dimensional dosimetry," *Med. Phys.* **24**, 223–231 (1997).

²⁴J. F. Dempsey, D. A. Low, S. Mutic, J. Markman, A. S. Kirov, G. H. Nussbaum, and J. F. Williamson, "Validation of a precision radiochromic film dosimetry system for quantitative two-dimensional imaging of acute exposure dose distributions," *Med. Phys.* **27**, 2462–2475 (2000).

²⁵M. J. Butson, K. N. Yu, T. Cheung, and P. E. Metcalfe, "Radiochromic film for Medical Radiation Dosimetry," *Mater. Sci. Eng., R.* **41**, 61–120 (2003).

²⁶S. D. Thomas, M. Mackenzie, G. C. Field, A. M. Syme, and B. G. Fallone, "Patient specific treatment verifications for helical tomotherapy treatment plans," *Med. Phys.* **32**, 3793–3800 (2005).